Chiral and achiral crystals, charge-assisted hydrogen-bond patterns and self-organization of selected solid diaminium thiosulfates

Agnieszka Brozdowska and Jarosław Chojnacki

Chiral and achiral crystals, charge-assisted hydrogen-bond patterns and self-organization of selected solid diaminium thiosulfates

Agnieszka Brozdowska* and Jarosław Chojnacki

Department of Inorganic Chemistry, Gdańsk University of Technology, G. Narutowicza 11/12, Gdańsk 80233, Poland. *Correspondence e-mail: brozdowska.agnieszka@gmail.com

A series of diaminium thiosulfates, derivatives of diamines: $NH_2CH_2CH(CH_3)NH_2$ (1) and $NH_2(CH_2)_nNH_2$, n = 3–6 [(2)–(5)] and thiosulfuric acid were prepared and their structures determined by single-crystal X-ray diffraction analysis. Compounds (1), (2) and (4) turned out to be hydrates. The crystal structure of 1,2-propylenediaminium thiosulfate is chiral and exhibits spontaneous resolution. Crystals for both enantiomers [(1a) and (1b)] were obtained with high enantiometric excess and examined. An extended network of strong, charge-assisted hydrogen bonding of the $^{+}N-H \cdots O^{-}$ type (also $O-H \cdots O$ and $O-H \cdots S$ for hydrates) is most likely the main factor defining crystal packing and the variable conformation of the cations. The formation of chiral hydrogen-bond motifs – distorted cubans – seems to induce the formation of chiral solid-state structure from achiral components in the case of (4). Diaminium thiosulfates with an odd number of C atoms in the alkyl chain [compounds (1), (2) and (4)] form three-dimensional supramolecular networks, while in the case of diaminium salts with an even number of C atoms [(3) and (5)], two-dimensional layers of hydrogen-bond domains are observed. The aminium thiosulfates were also characterized by elemental analysis, NMR and Fourier transform (FT)–IR spectroscopy. The conformations of α,ω-alkyl-diaminium cations in the solid state are discussed and rationalized by DFT calculations.

1. Introduction

Diamino aliphatic alkanes of the general formula NH_2RNH_2 (R = hydrocarbon chain) are compounds of basic character with enhanced reactivity with strong organic and inorganic acids. In the resulting salts both ammonium groups are usually protonated forming flexible dications which can create a network of hydrogen bonding with the counterions (Paul & Kubicki, 2010). Diaminium salts are commonly used as templating moieties in crystal engineering (Möller & Bein, 2013; Cheng & Lin, 2010; Yu *et al.*, 2014). α,ω-Alkyldiaminium cations with straight hydrocarbon chains C2—C12 are well known for their applications as linkers in a two-dimensional or three-dimensional structure formation of various inorganic organic nanocomposites (Lemmerer & Billing, 2012; Visi *et al.*, 2006; Önal & Sarıkaya, 2008), for example, for the preparation of thin film semiconductors (Mitzi, 2004). Flexible α,ω-alkyl-diamines could be used in molecular switches, as molecular 'transducers' in which the molecular lengths of the hydrocarbon chain of the complexed diaminium cation is transferred into a change in helical handedness of the host (Knipe *et al.*, 2015).

The packing in the solid state and conformational changes of the flexible alkyldiaminium cations in different systems
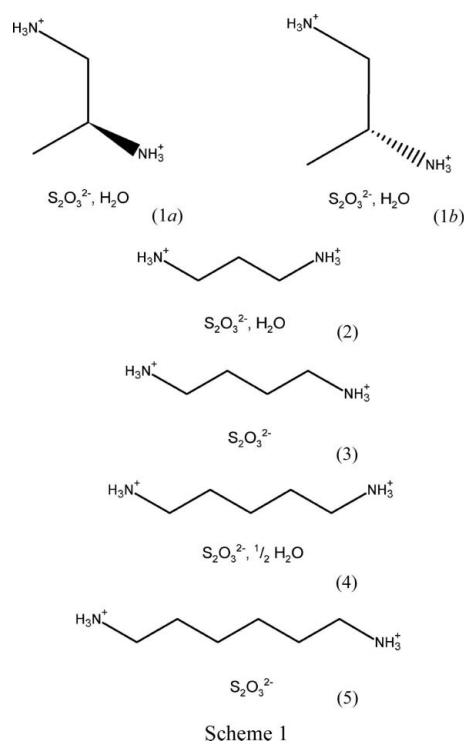
https://doi.org/10.1107/S2052520617004802

have been recently investigated both in solution (Dumitrescu *et al.*, 2014, 2015; Fang *et al.*, 2016) and in the solid state (Lemmerer & Billing, 2012; Visi *et al.*, 2006; Song *et al.*, 2002). A Cambridge Structural Database (Allen, 2002) overview of structures with 1,4-butanediaminium and 1,6-hexanediaminium cations was carried out by Paul and Kubicki in 2008 (Paul & Kubicki, 2009, 2010). The results of the current overview of the CSD (Version 5.37, February 2016) for diaminium cations $\{NH_3(CH_2)_nNH_3\}^{2+}$ (n = 3–6) and $\{NH_3(CH_2)_2NH_3CH_3\}^{2+}$ are presented in this work. We decided to examine the series of diaminium salts of thiosulfuric acid in order to reveal their supramolecular organization with a detailed description of hydrogen-bonding occurrence.

Although thiosulfates are commonly known in chemistry, their reactivity was mainly examined for the inorganic salts. By replacing the metal or ammonium cation with organic species we obtain compounds with new properties. Thiosulfates of protonated amines, which were often received by chance, have been the subject of merely a few publications (Leyten *et al.*, 1988; Yang & Ng, 2011; Jiang *et al.*, 1998; Srinivasan *et al.*, 2011; Okuniewski *et al.*, 2013; Seck *et al.*, 2016). Aminium thiosulfates are the focus of our research due to their interesting supramolecular organization in the solid state. Examination of their structure reveals important details regarding self-assembly in the solid state, hydrogen-bonding network topology and, additionally in some cases, shows that the crystals lack inversion centres and as such give non-centrosymmetric physical properties (*e.g.* generation of second harmonic wave or piezoelectricity; Srinivasan *et al.*, 2013). The hydrogen bonding plays a crucial role here in structure formation as it is enhanced by electric charges on both donor and acceptor groups and thus is energetically preferred. In some cases the enthalpy of formation can be close to regular covalent bonding (Lopes Jesus & Redinha, 2011). The hierarchy of hydrogen-bond energy among the structures of α,ω-alkyldiaminium thiosulfates is also discussed herein.

Alkyldiaminium thiosulfates are potentially interesting compounds because of the possibility to investigate the influence of the length and shape of the hydrocarbon chain on the structures. Until now, only two structures of alkyldiaminium thiosulfates have been published: ethylenediaminium thiosulfate $\{(H_3NC_2H_4NH_3)^{2+}, S_2O_3^{2-}\}$ (Srinivasan *et al.*, 2013) and salt with protonated 1,6-diaminohexane $\{2NH_4^+, (H_3NC_6H_{12}NH_3)^{2+}, 2S_2O_3^{2-}\}$ (Dąbrowska & Chojnacki, 2014). Herein, we present preparation and structural analysis for new members of this class of compounds: 1,2-propylenediaminium thiosulfate [structures (1*a*) and (1*b*)], 1,3-propylenediaminium thiosulfate (2), 1,4-butylenediaminium thiosulfate (3), 1,5-pentylenediaminium thiosulfate (4) and 1,6-hexylenediaminium thiosulfate (5) (Scheme 1). The preparation of (2) and (5) has previously been reported by us (Dąbrowska & Chojnacki, 2014), but the crystals produced at that time were not suitable for single-crystal X-ray diffraction analysis. In order to better understand the packing of diaminium salts in the solid state, DFT calculations for selected salts [(2) and (3)] were

conducted.

Scheme 1

2. Experimental

2.1. Materials and methods

Ammonium thiosulfate was received from Merck, 98%+ pure grade and used as such. Amines were purchased from different commercial sources and distilled before use. Solvents were of analytical pure grade and were received from Avantor. Obtained aminium thiosulfates were examined by elemental analyses at the Vario El Cube CHNS apparatus (Elementar, Germany). Melting points were determined by Melting point SMP30 (Stuart, UK). Measurements of the FT–IR spectra for crystalline compounds (1)–(3) and (5) were performed using an attenuated total reflection (ATR) accessory on a Nicolet 8700 spectrometer (Thermo Electron, USA) in the range 4500–500 cm^{-1}. For compound (4) the solid-state FT–IR spectrum was measured in the range 4000–400 cm^{-1} with a Nicolet iS50 spectrometer (ThermoScientific, USA) equipped with the Specac Quest (ATR) accessory. NMR spectra measurements were performed on a Bruker Avance III HD 400 MHz spectrometer (USA) with TXI ^{1}H/^{13}C/^{31}P probe.

2.2. Synthetic procedures

Diaminium thiosulfates were obtained in the reaction of ammonium thiosulfate with the corresponding diamine in aqueous solution as described by Srinivasan *et al.* (2011). The general procedure was as follows: both reagents were dissolved in water, the combined solutions were stirred for 15 min in a bath at room or elevated temperatures, then the contents were filtrated and evaporated to dryness. The crude

__

solid product was crystallized from a small portion of water or ethanol. Detailed synthetic procedures are described below.

2.2.1. 1,2-Propylenediaminium thiosulfate monohydrate. For the preparation of $C_3H_{14}N_2O_4S_2$ [(1*a*) and (1*b*)], (±)-1,2-diaminopropane (1.7 ml, 20 mmol) was dissolved in distilled water (10 ml) and then added to 10 ml of water solution of ammonium thiosulfate (2.97 g, 20 mmol). The reaction mixture was heated at 353 K for 15 min, filtered and evaporated. The crude product was crystallized from a small amount of water in a heated bath at 328 K and left to evaporate slowly at room temperature. Elemental analysis: found: C 17.55, H 6.9, N 13.4, S 31.0; calc. for monohydrate $C_3H_{14}N_2O_4S_2$: C 17.5, H 6.8, N 13.6, S 31.1%; m.p. 474–476 K (with decomposition). IR: ν_{max} (cm^{-1}) 3380 and 3345 (νNH), 2930 (νCH), 1626 and 1595 (δNH), 1076 and 1061 (νCN), 974 (ν_sSO$_3$), 667 (δSO$_3$), 534 (ν_{as}SO$_3$). ^{1}H NMR (400 MHz) in D$_2$O: 1.35 (3H, d, Me), 3.18 and 3.32 (1H and 1H, dd and dd, CH$_2$), 3.71 (1H, sex, CH), 4.69 (6H, s, NH$_3^+$). ^{13}C (100 MHz) in D$_2$O: 15.5 (Me), 42.0 and 45.0 (CH$_2$ and CH).

2.2.2. 1,3-Propylenediaminium thiosulfate monohydrate. $C_3H_{14}N_2O_4S_2$ (2) was obtained by mixing a solution of 1,3-diaminopropane (1.3 ml, 20 mmol) in distilled water (10 ml) with 10 ml of a water solution of ammonium thiosulfate (2.964 g, 20 mmol). The reaction mixture was heated at 353 K for 15 min, filtered and evaporated resulting in 3.378 g of crude product, 89% yield. Crude product was crystallized from 25 ml of water–ethanol solution (4:1 volume ratio) and left to evaporate slowly at room temperature. Elemental analysis: found: C 17.2, H 6.6, N 13.2, S 29.6; calc. for monohydrate $C_3H_{14}N_2O_4S_2$: C 17.5, H 6.8, N 13.6, S 31.1%; m.p. 493–496 K (decomp.). IR: ν_{max} (cm^{-1}) 3402 and 3373 (νNH), 2890 (νCH), 1601 and 1597 (δNH), 1495 (δCH), 1070 (νCN), 980 (ν_sSO$_3$), 658 (δSO$_3$), 530 (ν_{as}SO$_3$). ^{1}H NMR (400 MHz) in D$_2$O: 1.99 (2H, p, CCH$_2$C), 3.02 (4H, dd, CCH$_2$N), 4.70 (6H, s, NH$_3^+$). ^{13}C (100 MHz) in D$_2$O: 25.0 (CCH$_2$C), 36.5 (CCH$_2$N).

2.2.3. 1,4-butylenediaminium thiosulfate. For the preparation of $C_4H_{14}N_2O_3S_2$ (3), 1,4-diaminobutane (1.763 g, 20 mmol) was dissolved in distilled water (44 ml) and added to 10 ml of a water solution of ammonium thiosulfate (2.964 g, 20 mmol). The reaction mixture was mixed using a magnetic stirrer for 15 min, filtered and left to evaporate slowly at room temperature. After a few weeks well formed, colourless crystals of (3) were obtained. Elemental analysis: found: C 23.7, H 6.9, N 13.7, S 31.9; calc. for $C_4H_{14}N_2O_3S_2$: C 23.75, H 7.0, N 13.85, S 31.7%; m.p. 465 K (decomp.). IR: ν_{max} (cm^{-1}) 3330 (νNH), 2939 (νCH), 1612 (δNH), 1510 and 1496 (δCH), 1092 (νCN), 987 (ν_sSO$_3$), 663 (δSO$_3$), 538 (ν_{as}SO$_3$). ^{1}H NMR (400 MHz) in D$_2$O: 1.63 (4H, p, CCH$_2$C), 2.92 (4H, t, CCH$_2$N), 4.70 (6H, s, NH$_3^+$). ^{13}C (100 MHz) in D$_2$O: 24.0 (CCH$_2$C), 39.0 (CCH$_2$N).

2.2.4. 1,5-Pentylenediaminium thiosulfate hemihydrate. $C_5H_{18}N_2O_4S_2$ (4) was prepared by mixing a water solution (5 ml) of 1,5-diaminopentane (1.5 ml, 13 mmol) with 5 ml of a water solution of ammonium thiosulfate (1.911 g, 13 mmol). The reaction mixture was heated at 313 K for 1.5 h, filtered and vacuum evaporated resulting in a light-yellow crystalline precipitate in the oily liquid. The precipitate with oil was

then crystallized from cold water (5 ml); the resulting solution had a yellow colour and was left to evaporate slowly at room temperature. The solution went dark-brown but after 4 months thin, needle-shape crystals of (4) formed. Elemental analysis: found: C 25.6, H 7.4, N 11.9, S 28.35; calc. for hemihydrate $C_5H_{16}N_2O_3S_2 \cdot \frac{1}{2}H_2O$: C 26.6, H 7.6, N 12.4, S 28.5%; m.p. 465–467 K (decomp.). IR: ν_{max} (cm^{-1}) 3520 (νNH), 2900 (νCH), 1616 (δNH), 1507 and 1458 (δCH), 1081 (νCN), 980 (ν_sSO$_3$), 656 (δSO$_3$), 532 (ν_{as}SO$_3$). ^{1}H NMR (400 MHz) in D$_2$O: 1.37 (2H, p, central CH$_2$), 1.62 (4H, p, CCH$_2$C), 2.93 (4H, t, CCH$_2$N), 4.69 (6H, s, NH$_3^+$). ^{13}C (100 MHz) in D$_2$O: 22.5 (central CH$_2$), 26.0 (CCH$_2$C), 39.0 (CCH$_2$N).

2.2.5. 1,6-Hexylenediaminium thiosulfate. $C_6H_{18}N_2O_3S_2$ (5) was obtained by mixing a water solution (10 ml) of 1,6-diaminohexane (2.324 g, 20 mmol) with 10 ml of a water solution of ammonium thiosulfate (2.964 g, 20 mmol). The reaction mixture was heated at 353 K for 15 min, filtered and left to evaporate slowly at room temperature. Elemental analysis: found: C 30.9, H 7.8, N 12.0, S 27.8; calc. for $C_6H_{18}N_2O_3S_2$: C 31.3, H 7.9, N 12.2, S 27.8%; m.p. 467–470 K (decomp.). IR: ν_{max} (cm^{-1}) 2937 (νCH), 1610 (δNH), 1510 and 1504 (δCH), 1080 (νCN), 985 (ν_sSO$_3$), 669 (δSO$_3$), 536 (ν_{as}SO$_3$). ^{1}H NMR (400 MHz) in D$_2$O: 1.30 (4H, p, central CH$_2$), 1.57 (4H, p, CCH$_2$C), 2.89 (4H, t, CCH$_2$N), 4.70 (6H, s, NH$_3^+$). ^{13}C (100 MHz) in D$_2$O: 25.0 (central CH$_2$), 26.5 (CCH$_2$C), 39.5 (CCH$_2$N).

2.3. Single-crystal X-ray diffraction

X-ray analyses were carried out using KUMA KM4 CCD [structures (1)–(3)] or Stoe IPDS instruments [(4)–(5)].

KUMA: Diffraction data were recorded at 120.0 (2) K or at room temperature 293.0 (2) K on a KUMA KM4 (Wrocław, Poland) diffractometer with graphite-monochromated Mo $K\alpha$ radiation (0.71073 Å), equipped with a Sapphire 2 CCD camera (Oxford Diffraction, Yarnton, England). Data collection was performed using *CrysAlisPro* (Agilent Technologies, 2013) in the ω-scan mode. Analytical absorption correction was applied for all strongly absorbing crystals.

Stoe: Diffraction intensity data were collected on an IPDS 2T dual-beam diffractometer (Stoe & Cie GmbH, Darmstadt, Germany) at 120.0 (2) K with Mo $K\alpha$ radiation of a microfocus X-ray source (GeniX 3D Mo High Flux, Xenocs, Sassenage, 50 kV, 1.0 mA, λ = 0.71069 Å). The crystal was thermostated in a nitrogen stream at 120 K using a Cryo-Stream-800 device (Oxford CryoSystem, UK) during the entire experiment. Data collection and reduction were controlled by *X-Area*1.75 (Stoe, 2015). An absorption correction was performed on the integrated reflections by a combination of frame scaling, reflection scaling and a spherical absorption correction. Outliers have been rejected according to Blessing's method (Blessing, 1997).

Structures were solved using direct methods with *SHELXS*13 and refined using full-matrix least-squares refinement based on F^2 by *SHELXL*2014 (Sheldrick, 2008) run under the control of *WinGx* (Farrugia, 2012). All non-H atoms were refined as anisotropic. A summary of crystal-

Table 1
Experimental details.

	(1a)	(1b)	(2)
Crystal data			
Chemical formula	$O_3S_2^{2-}\cdot C_3H_{12}N_2^{2+}\cdot H_2O$	$O_3S_2^{2-}\cdot C_3H_{12}N_2^{2+}\cdot H_2O$	$O_3S_2^{2-}\cdot C_3H_{12}N_2^{2+}\cdot H_2O$
M_r	206.28	206.28	206.28
Crystal system, space group	Orthorhombic, $P2_12_12_1$	Orthorhombic, $P2_12_12_1$	Monoclinic, $P2_1/n$
Temperature (K)	293	120	120
a, b, c (Å)	8.4086 (5), 9.7870 (5), 11.0477 (6)	8.3714 (6), 9.7607 (10), 10.9874 (12)	15.4097 (8), 8.0868 (4), 15.4133 (13)
β (°)	90	90	108.249 (6)
V (Å^3)	909.17 (9)	897.79 (15)	1824.1 (2)
Z	4	4	8
Radiation type	Mo $K\alpha$	Mo $K\alpha$	Mo $K\alpha$
μ (mm^{-1})	0.56	0.57	0.56
Crystal size (mm)	$0.52 \times 0.34 \times 0.12$	$0.41 \times 0.35 \times 0.2$	$0.37 \times 0.09 \times 0.07$
Data collection			
Diffractometer	KUMA KM4CCD, Sapphire2, large Be window	KUMA KM4CCD, Sapphire2, large Be window	KUMA KM4CCD, Sapphire2, large Be window
Absorption correction	Multi-scan *CrysAlisPro*	Multi-scan *CrysAlisPro*	Multi-scan *CrysAlisPro*
T_{min}, T_{max}	0.890, 1	0.752, 1	0.913, 1
No. of measured, independent and observed [$I > 2\sigma(I)$] reflections	3135, 1620, 1497	2086, 1506, 1361	5760, 3262, 2918
R_{int}	0.032	0.027	0.025
$(\sin\theta/\lambda)_{max}$ (Å^{-1})	0.597	0.597	0.606
Refinement			
$R[F^2 > 2\sigma(F^2)]$, $wR(F^2)$, S	0.038, 0.093, 1.06	0.044, 0.108, 1.04	0.045, 0.120, 1.05
No. of reflections	1620	1506	3262
No. of parameters	108	109	219
No. of restraints	2	0	4
H-atom treatment	H atoms treated by a mixture of independent and constrained refinement	H atoms treated by a mixture of independent and constrained refinement	H atoms treated by a mixture of independent and constrained refinement
$\Delta\rho_{max}, \Delta\rho_{min}$ (e Å^{-3})	0.40, −0.22	0.51, −0.35	0.63, −0.44
Absolute structure	Flack x determined using 577 quotients $[(I^+) - (I^-)]/[(I^+) + (I^-)]$ (Parsons *et al.*, 2013)	Refined as an inversion twin	–
Absolute structure parameter	−0.09 (9)	−0.2 (2)	–

	(3)	(4)	(5)
Crystal data			
Chemical formula	$C_4H_{14}N_2^{2+}\cdot O_3S_2^{2-}$	$C_5H_{16}N_2^{2+}\cdot O_3S_2^{2-}\cdot 0.5(O)$	$C_6H_{18}N_2^{2+}\cdot O_3S_2^{2-}$
M_r	202.29	224.32	230.34
Crystal system, space group	Triclinic, $P\bar{1}$	Tetragonal, $P4_32_12$	Triclinic, $P\bar{1}$
Temperature (K)	120	120	120
a, b, c (Å)	6.0538 (5), 8.5273 (6), 9.3869 (8)	11.7872 (9), 11.7872 (9), 16.2851 (14)	10.4922 (10), 11.1455 (11), 11.7015 (12)
α, β, γ (°)	73.623 (7), 82.681 (7), 84.207 (7)	90, 90, 90	62.299 (7), 74.938 (8), 74.082 (8)
V (Å^3)	460.05 (7)	2262.6 (4)	1150.9 (2)
Z	2	8	4
Radiation type	Mo $K\alpha$	Mo $K\alpha$	Mo $K\alpha$
μ (mm^{-1})	0.55	0.45	0.45
Crystal size (mm)	$0.56 \times 0.41 \times 0.33$	$0.36 \times 0.06 \times 0.04$	$0.31 \times 0.22 \times 0.15$
Data collection			
Diffractometer	KUMA KM4CCD, Sapphire2, large Be window	Stoe IPDS 2T	Stoe IPDS 2T
Absorption correction	Multi-scan *CrysAlisPro*	–	–
T_{min}, T_{max}	0.775, 1	–	–
No. of measured, independent and observed [$I > 2\sigma(I)$] reflections	2675, 1786, 1416	15 572, 2008, 1762	4093, 4093, 3644
R_{int}	0.031	0.076	0.114
$(\sin\theta/\lambda)_{max}$ (Å^{-1})	0.617	0.597	0.597
Refinement			
$R[F^2 > 2\sigma(F^2)]$, $wR(F^2)$, S	0.053, 0.134, 1.06	0.059, 0.167, 1.03	0.078, 0.239, 1.17
No. of reflections	1786	2008	4093
No. of parameters	124	117	240
No. of restraints	6	0	0

Table 1 (continued)

	(3)	(4)	(5)
H-atom treatment	H atoms treated by a mixture of independent and constrained refinement	H-atom parameters constrained	H-atom parameters constrained
$\Delta\rho_{max}$, $\Delta\rho_{min}$ (e Å^{-3})	0.57, −0.52	0.90, −0.68	1.17, −1.35
Absolute structure	–	Flack x determined using 669 quotients $[(I^+) - (I^-)]/[(I^+) + (I^-)]$ (Parsons *et al.*, 2013)	–
Absolute structure parameter	–	0.00 (13)	–

Computer programs: *CrysAlisPro* (Agilent Technologies, 2011), *X-AREA*, *X-RED* (Stoe & Cie, 2015), *SHELXS*2013, *SHELXS*2014, *SHELXL*2014 (Sheldrick, 2008), *ORTEP* for Windows (Farrugia, 2012), *WinGX* publication routines (Farrugia, 2012).

lographic analyses for (1*a*), (1*b*), (2), (3), (4) and (5) is given in Table 1. Hydrogen bonding parameters are gathered in the supporting information (Tables S1–S6). Figures were generated using *Mercury* (Macrae *et al.*, 2008) and *ChemSketch* (Hunter, 1997).

2.3.1. Refinement. C-bound H atoms were refined in geometrically idealized positions with isotropic temperature factors 1.2 or 1.5 times the equivalent isotropic temperature factors, U_{eq}, of their attached atoms. The N—H and O—H hydrogen atoms were found in the difference-Fourier electron-density map and were refined with constraints or refined using the riding model. In the case of (4) H atoms at the disordered water molecule were not located. The structure of (1*b*) was refined as an inversion twin. The structure of (2) was refined as a two-component merohedral twin. The structure of (5) was refined as a pseudomerohedral twin with two components (using the HKLF 5 file generated by the *Twin-RotMat* program, with 635 overlap reflections out of 4097).

2.4. Quantum chemistry calculations

To study conformational stability we used potential energy surface (PES) scans performed by *GAUSSIAN*09W (Frisch *et al.*, 2009) at the B3LYP/6-31+G theory level. It is a series of energy calculations conducted for molecules with one internal coordinate (the torsion angle in our case) restricted to a set value. The scans were performed in the relaxed mode, so at every point the rest of the molecule (except the frozen fragment) was free to adopt its optimal shape. After setting the torsion of interest, we optimize the geometry. When the molecule achieves the minimum energy, the torsion is set to the next value (usually with increments of 10°) and the process repeated, until the whole range of torsions is done. Having these data a diagram of 'energy–torsion' can be constructed. Models of cations were loaded from experimental data and bond lengths to H atoms were normalized to their more realistic values using *Mercury* (Macrae *et al.*, 2008).

The model for molecular calculations of 1,3-propylenediaminium cation was loaded from the experimental data of (2) (N3–N4 cation) and models of both cation conformations for molecular calculations of 1,4-butylenediamonium cations were loaded from the experimental data of (3), where the central C atoms have a zigzag conformation.

3. Results and discussion

3.1. Crystal structures

Details of the solid-state structures of the diaminium thiosulfates obtained are discussed below.

3.1.1. 1,2-Propylenediaminium thiosulfate hydrate. Compound (1) crystallizes as a monohydrate in the space group $P2_12_12_1$, which belongs to Sohncke space groups. These are 65 space groups that comprise only rotation or screw axes and are the only space groups chiral structures can crystallize in. Despite 1,2-diaminopropane having a stereogenic centre at the C2 atom, its salts rarely crystallize in Sohncke space groups due to the use of the racemic substrate, and spontaneous separation of the enantiomers usually does not occur during the crystallization. Among 111 structures with the 1,2-propylenediaminium dication deposited at the Cambridge Structural Database (CSD Version 5.37, last update February 2016), only eight belong to Sohncke space groups (Wong *et al.*, 2015; Zhou *et al.*, 2015; Zheng *et al.*, 2008; Budantseva *et al.*, 2003; Armstrong *et al.*, 2002; Bu *et al.*, 1998; Feng *et al.*, 1998). There are 96 (86.5%) organometallic structures and only 15 (13.5%) among the deposited compounds are organic and simple inorganic salts with the 1,2-propylenediaminium dication.

Moreover, simple salts of 1,2-diaminopropane such as those with tetrahedral anions: $[HPO_4]^{2-}$ (space group $P2_1/n$) (Baouab & Jouini, 1998), $[HAsO_4]^{2-}$ ($P2_1/n$) (Lee & Harrison, 2003; Todd & Harrison, 2005), $[SO_4]^{2-}$ ($P2_1/n$) (Guerfel & Jouini, 2000), $[BeF_4]^{2-}$ ($P2_1/n$) (Gerrard & Weller, 2002), $[CrO_4]^{2-}$ ($P2_1/c$) (Trabelsi *et al.*, 2014) or propane-1,2-diaminium dichloride ($Pna2_1$; Pospieszna-Markiewicz *et al.*, 2011) all crystallize as racemates.

It has been reported that ethylenediaminium thiosulfate also crystallized in the Sohncke space group (Srinivasan *et al.*, 2013). Although $H_3NC_2H_4NH_3S_2O_3$ does not contain any stereogenic centre and both the unique ethylenediaminium cations adopt an *anti* conformation, it forms chiral crystals and as such exhibits the second harmonic generation (SHG) property appearing as a green light emission generated from a beam of IR. It is noteworthy that also some achiral salts of protonated 1,2-diaminoethane with tetrahedral anions $[SO_4]^{2-}$, $[BeF_4]^{2-}$, $[CrO_4]^{2-}$, $[MoS_4]^{2-}$, $[WS_4]^{2-}$, $[ZnCl_4]^{2-}$ crystallize in Sohncke space groups in contrast to the corresponding 1,2-propylenediaminium salts.

In our research we managed to obtain and select crystals of both enantiomers S-1,2-propylenediaminium thiosulfate [(1a); Fig. 1] and R-1,2-propylenediaminium thiosulfate (1b) as reaction products of the racemic 1,2-diaminopropane. The absolute structure Flack parameter is close to zero [−0.09 (9)] for the (1a) structure, which confirms the correctness of the solution. In the case of structure (1b), the absolute structure Flack parameter is higher [−0.2 (2)], which indicates that it crystallizes as a conglomerate with the 62% enantiomeric excess of the R-1,2-propylenediaminium thiosulfate enantiomer. Unit-cell parameters for both structures are insignificantly different due to the fact that diffraction experiments were carried out at different temperatures (Table 1). Electrically charged N atoms are located in the *anti* position (torsion angle N1—C1—C2—N2 *ca* 160°) in the cation. Extensive hydrogen bonding of the N—H$\cdots$O and O—H$\cdots$S type interlinks ions and water molecules into a three-dimensional supramolecular structure. Protonated amine groups form strong charge-assisted hydrogen bonds of the $^+$N—H$\cdots$O$^-$ type only to O atoms: N2 with two O atoms from the thiosulfate group (O2 and O3) and one from the water molecule (O4), while H atoms on N1 form bonds with three anionic O atoms (O1, O2 and O3 all from different entities). The water molecule acts as a hydrogen bond donor to the remaining acceptors, *i.e.* one anionic oxygen atom (O1) and one anionic sulfur atom (S2). Noteworthy, N—H$\cdots$S bonds are not formed, probably due to the hierarchy of bonding energy for NH groups $^+$N—H$\cdots$O$^-$ > $^+$N—H$\cdots$S$^-$ and for OH groups O—H$\cdots$O$^-$ > O—H$\cdots$S$^-$. The H atoms form intermolecular hydrogen bonds without bifurcation. The smallest ring motifs are $R_3^3(11)$, $R_4^4(12)$ and $R_3^3(13)$, where $R_D^A(N)$ denotes: D – number of donors, A – acceptors, N – ring size (for graph set notation see Bernstein *et al.*, 1995).

3.1.2. 1,3-Propylenediaminium thiosulfate hydrate.
Compound (2) crystallizes as a monohydrate in the monoclinic system in the $P2_1/n$ space group. The asymmetric unit of (2) consists of two thiosulfate anions, two different [NH$_3$(CH$_2$)$_3$NH$_3$]$^{2+}$ cations and two molecules of water. The structure of (2) is shown in Fig. 2. One 1,3-propylenediaminium cation adopts a zigzag conformation in which both electrically charged N atoms are located in the antiperiplanar *ap*, *ap* positions, while in the second cation one of the torsion angles is synclinal (torsion angle N3—C4—C5—C6 *ca* −64°), indicating the *ap*, *sc* conformation. Separation of repelling N atoms is 4.975 (4) and 4.522 (5) Å, for N1$\cdots$N2 and N3$\cdots$N4, respectively. The stability of the second conformation most likely results from intermolecular interactions in the solid state. Distances of terminal C atoms are: 2.473 (6) and 2.549 (5) Å for C1$\cdots$C3 and C4$\cdots$C6, respectively. It is noteworthy that the larger N$\cdots$N separation is related to the smaller C$_\alpha\cdots$C$_\omega$ separation.

Generally, 1,3-propylenediaminium cations in the solid state can adopt three main conformations depending on the two torsion angles at heavy atoms (first: N1—C1—C2—C3 and second: C1—C2—C3—N2). In the first conformation both ammonium groups are located in antiperiplanar positions (*ap*, *ap*), in the second case one torsion angle is approximately 180°, while the second torsion is synclinal (*ap*, *sc*), in the third possibility the cation has two synclinal torsion angles (*sc*, *sc*). In the supporting information the histogram (Fig. S1) demonstrates the distribution of torsion angles among the structures of 1,3-diaminopropane salts deposited in the CSD crystallographic database (Version 5.37, February 2016). It reveals that the most preferable NH$_3$(CH$_2$)$_3$NH$_3$ cation conformation is (*ap*, *ap*), the zigzag form, while structures with two ammonium groups in synclinal positions are the least favourable. Our DFT calculations conducted with the *GAUSSIAN*09W program confirm the conformational preferences and show that the difference between the energy of 1,3-propylenediaminium cation with *ap*, *ap* (zigzag) conformation and the one with *ap*, *sc* torsion angles is small, approximately 16.7 kJ mol^{-1} (4 kcal mol^{-1}).

Fig. 3 shows the dependence of the total energy of the cation on the torsion angle of one protonated ammonium group. At every calculation point the second ammonium group was free to adopt its optimal position, however, it
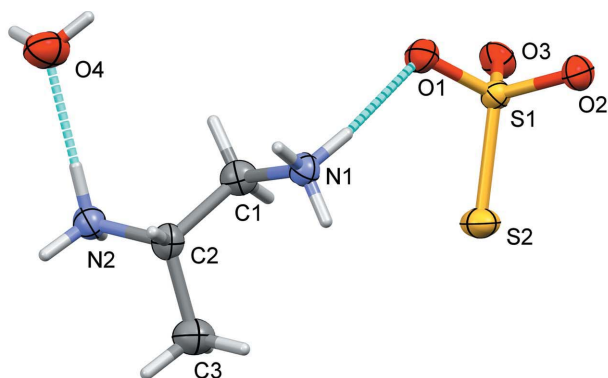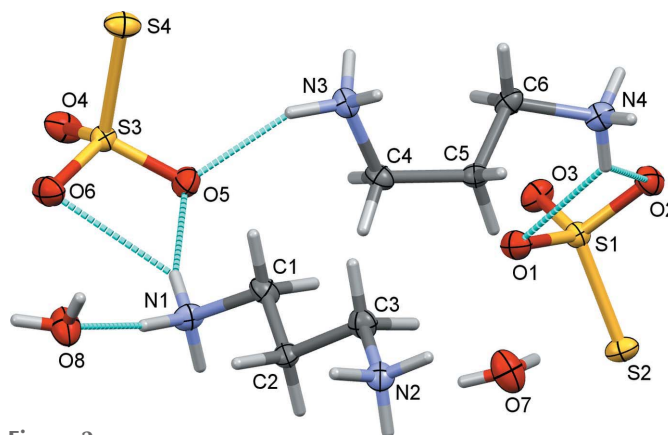

Figure 1
Molecular structure and atom-labelling scheme of 1,2-propylenediaminium thiosulfate (1a). Hydrogen bonds shown as dotted lines. Hanging hydrogen bonds are deleted. Ellipsoids drawn at the 50% probability level.

Figure 2
Molecular structure and atom-labelling scheme of 1,3-propylenediaminium thiosulfate (2). Hydrogen bonds shown as dotted lines. Hanging hydrogen bonds are deleted. Ellipsoids drawn at the 50% probability level.

remained in the *ap* position in the range ±(168–180°) during the whole study (Fig. S2).

One 1,3-propylenediaminium cation being the less energetically favourable form might be explained by the formation of a more stable hydrogen-bonding network in the crystal of (2). All H atoms from ammonium groups and water molecules are taking part in a hydrogen-bonding network. Again, charge-assisted $^+$N—H···O$^-$ bonds are formed wherever possible. Bonding of both water molecules is analogous as previously in (1) having both acceptor and donor character. The O atom is a hydrogen-bond acceptor from the protonated amine group, and the H atoms form O—H···O$^-$ and O—H···S$^-$ bonds with the thiosulfate groups. This time we can find two N2—H2C···S2^v [(v) $-x + \frac{1}{2}, y + \frac{1}{2}, -z + \frac{1}{2}$; the numbering of the symmetry codes are the same as in the hydrogen-bond geometry tables in the supporting information] and N3—H3C···S2^{vi} [(vi) $-x + \frac{1}{2}, y - \frac{1}{2}, -z + \frac{1}{2}$] interactions but this is of secondary importance being part of the bifurcated hydrogen bond. The hydrogen-bonding network forms a supramolecular three-dimensional structure including a number of cyclic motifs. The smallest ring motifs in (2) are $R_4^2(8)$ based on N4, O2^{viii}, N4^a, O2^{ix} [(a) $-x, -y, -z$] and N1, O5, N1^{iii}, O5^{iii} (two ammonium groups and two anion oxygen atoms) and lie on symmetry centres of the crystal (0 0 0) and ($\frac{1}{2}$ $\frac{1}{2}$ 0) and their equivalents, respectively. Moreover, $R_4^4(12)$ motifs are formed from N3 ammonium groups and thiosulfate anions (with O4 and O5 acceptor atoms) and their symmetry equivalents about another symmetry centre at ($\frac{1}{2}$ 0 0). Definitely the formation of many strong hydrogen bonds compensate for the energy loss required for the existence of the less stable conformer of the cation.
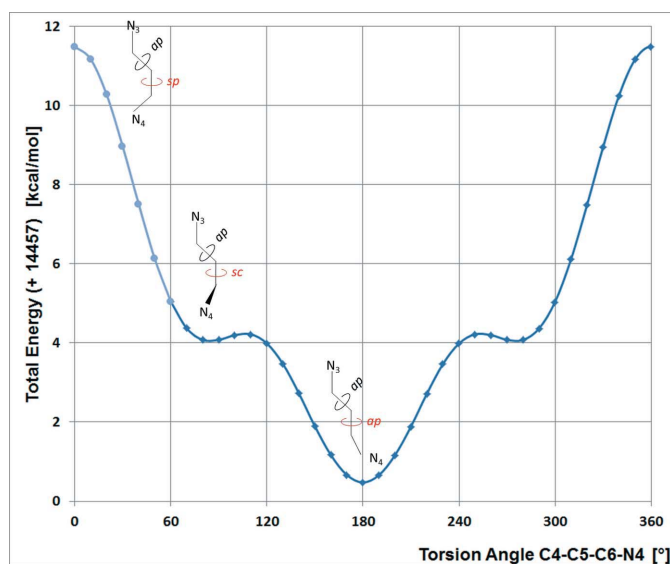
Crystals of (2) exhibit an interesting type of twinning. Since the lengths of sides *a* and *c* are very similar (see Table 1) there are two orientations of unit cells where these two parameters are interchanged (TWIN matrix [001, 010, 100]). We repeated the diffraction measurement thrice and obtained three different proportions of twinning. The contribution of the first domain is 0.7512 (2) for the presented structure of (2), 0.248 (2) from the second experiment and 0.473 (2) for the last measurement.

3.1.3. 1,4-Butylenediaminium thiosulfate. Compound (3) crystallizes as an anhydrous salt in the $P\overline{1}$ (triclinic) space group. The asymmetric unit of (3) consists of half of one independent 1,4-butylenediaminium cation, half of a second independent [NH$_3$(CH$_2$)$_4$NH$_3$]$^{2+}$ independent cation and one thiosulfate anion (Fig. 4). Both cations are centrosymmetric *i.e.* obey point group $\overline{1}$ symmetry (C_i Schoenflies). Due to this, the three torsion angles, which can be defined for heavy atoms of a cation, are restrained. The central torsion is necessarily 180° (*ap*) and the terminal torsions have the same magnitude, but different sign. So in the first instance of the 1,4-butylenediaminium cation the two protonated ammonium groups adopt the (*ap*, *ap*, −*ap*) conformation (with terminal torsion angle *ca* ±178°), while in the second both terminal torsion angles are synclinal (*sc*, *ap*, −*sc*) (*ca* ±60°). It gives an N atom separation of 6.328 (7) Å for N1···N1^a (*a*: $-x + 1, -y, -z + 1$) and 5.325 (7) Å for N2···N2^b (*b*: $-x + 1, -y, -z$) and C$_\alpha$···C$_\omega$ separations of 3.885 (8) and 3.921 (8) Å, for C2···C2^a and C4···C4^b, respectively. Obviously, at longer separations the differences in energy of repulsion become smaller. In this case again, as for compound (2), a larger N···N distance is associated with the smaller C$_\alpha$···C$_\omega$ distance.

Each H atom from the ammonium groups takes part in a hydrogen-bonding network, forming a three-dimensional supramolecular structure. The structure does not contain
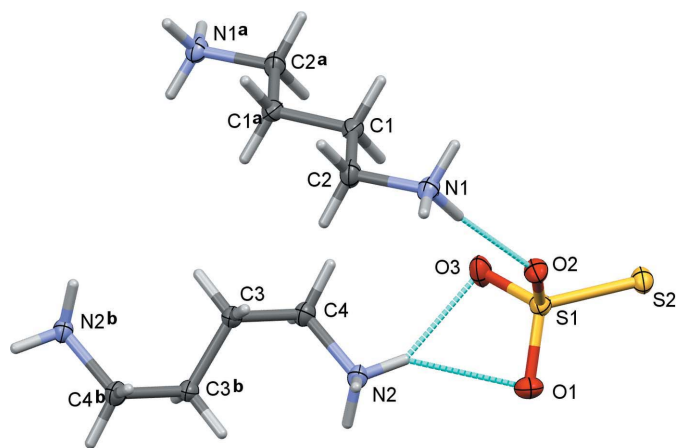

Figure 3
DFT relaxed potential energy surface (PES) scan, details in text. Dependence of the total energy on the restrained torsion of one protonated aminium group in the 1,3-propylenediaminium cation taken from structure (2). The red colour denotes the scanned torsion angle.

Figure 4
Molecular structure and atom-labelling scheme of 1,4-butylenediaminium thiosulfate (3), symmetry operation codes: (*a*) $-x + 1, -y, -z + 1$; (*b*) $-x + 1, -y, -z$. Hydrogen bonds shown as dotted lines. Hanging hydrogen bonds are deleted. Ellipsoids drawn at the 50% probability level.
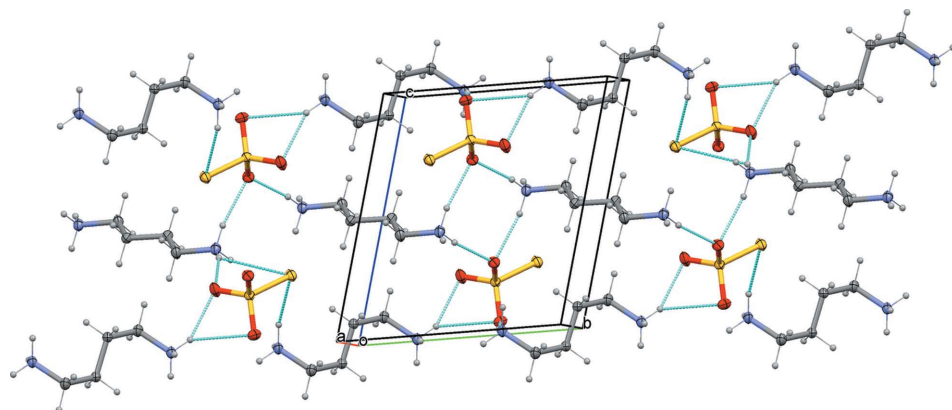
Figure 5
Packing diagram for (3). Alternate layered regions of hydrogen bonds and C—H chains are vertical in this projection, *i.e.* along the (010) plane.

water molecules, so after utilization of all $^+$N—H$\cdots$O$^-$ type, one $^+$N—H$\cdots$S$^-$ bond is formed N2—H2$M\cdots$S2^{iv} [(iv) $-x$, $-y+1$, $-z$]. The N1 of the ammonium group interacts with O2, O2^i and O3^{ii}. The first two interactions are organized into a cyclic motif $R_4^2(8)$ located at the symmetry centre ($\frac{1}{2}\frac{1}{2}\frac{1}{2}$). N2 of the other ammonium groups with O1 and O1^{iii} atoms also form a cyclic hydrogen bond motif $R_4^2(8)$ about a symmetry centre ($\frac{1}{2}\frac{1}{2}$ 0) and equivalent places. The overall structure can be rationalized as composed of plane regions of hydrogen bonding, parallel to (0 1 0), dominating at $y \in$ (0.3, 0.7) and regions where only hydrocarbon chains are present at $y \in$ (−0.3, 0.3) (Fig. 5).

Calculations of the total energy of the 1,4-butylenediaminium cation in different conformations were performed using the same methodology as for (2). We carried out three scans: for (N1—C2—C1—C1^a) torsion and the **ap**, ap, −ap conformer, for the (N2—C4—C3—C3^b) torsion and **sc**, ap, −sc conformer, and for the central torsion (C2—C1—C1^a—C2^a) and ap, **ap**, −ap conformer. In the first case (TOR1; scan torsion is indicated by bold font) the plot is symmetric with a minimum at TOR1 = 180° (Fig. S3a). The scan was performed in the relaxed mode, so at every point the second ammonium group could adopt its optimal position (TOR2), although it remained in the ap position [precisely it was ca −180° for TOR1 ∈(−180–0°) and ca 180° for TOR1 ∈(0–180°)]. The energy difference between the cation with ap, ap, −ap conformation and cation with sc, ap, −ap conformation is approximately 16.7 kJ mol^{-1} (4 kcal mol^{-1}). For the second case: starting with the sc, ap, −sc cation we obtained slightly different asymmetric results. The total energy difference between 1,4-butylenediaminium cation and −sc, ap, −sc conformation and the one with sc, ap, −sc torsion angles is approximately 8.4 kJ mol^{-1} (2 kcal mol^{-1}; Fig. S3b). The second terminal torsion angle (TOR2) in this cation remained synclinal for the whole calculations, *i.e.* remained between −69 and −82°. The third study investigated the total energy calculated as a function of the torsion angle of the central C atoms (Fig. S3c). In this case the energy difference between ap, ap, −ap and ap, sc, −ap conformations is approximately

12.6 kJ mol^{-1} (3 kcal mol^{-1}). Calculations confirm that the fully extended conformation of the 1,4-butylenediaminium cation is the most energetically favourable, however, the energy difference is small enough that the hydrogen-bond network can stabilize the less preferred conformation.

In the Cambridge Structural Database (Version 5.37, February 2016) there are 232 structures with the 1,4-butylenediaminium cation (164 with three-dimensional parameters defined). There are 146 (63%) organometallic structures, 48 (21%) organic and 38 (16%) simple inorganic salts with the 1,4-diaminobutane dication. To consider the shape of the α,ω-alkyldiaminium cation the N$\cdots$N separation can be measured. However, the C$_\alpha\cdots$C$_\omega$ distance is a better indicator of deviation from the linearity of the alkyl chain as it could be linear, but terminal ammonium groups could rotate (Visi *et al.*, 2006). Among the structures with the 1,4-butylenediaminium cation, 27 have more than one cation in the asymmetric unit, two of them are structures with different alkyl chain folding of independent cations and 19 with different conformations of independent cations when N$\cdots$N separation is considered. Only 17 (8.5%) structures have a fourth C atom in a *gauche* position and the rest of the structures have a fully extended linear carbon alkyl chain. A histogram of the conformations of the 1,4-diaminobutane dications in the CSD (Version 5.37, February 2016) is given in Fig. S4. It demonstrates that the vast majority of 1,4-butylenediaminium cations have a fully extended conformation, while twice fewer cations have an sc, ap, −sc conformation and the other conformation options are even less common.

3.1.4. 1,5-Pentylenediaminium thiosulfate hemihydrate. Compound (4) crystallizes in the $P4_32_12$ space group (Sohncke type) as the hemihydrate of the general formula: $\{(H_3NC_5H_{10}NH_3)^{2+}, S_2O_3^{2-}, \frac{1}{2}H_2O\}_n$. The asymmetric unit contains one entity of each type: cation, anion and half (disordered) water molecule. Cations adopt the most stable all
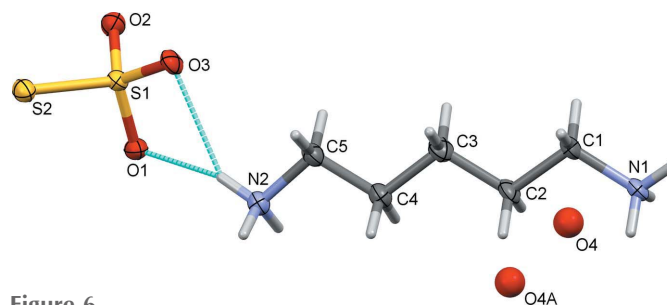

Figure 6
Molecular structure and atom-labelling scheme of 1,5-pentylenediaminium thiosulfate (4). Hydrogen bonds shown as dotted lines. Hanging hydrogen bonds are deleted. Ellipsoids drawn at the 50% probability level.

antiperiplanar (zigzag) conformation (Fig. 6). The separation of N atoms N1$\cdots$N2 is 7.408 (8) Å and the distance between terminal C atoms is 5.050 (9) Å.

As in the previous structures all H atoms from the protonated amine groups are involved in hydrogen bonding of the $^+$N—H$\cdots$O$^-$ type. In the structure of (4) there are two hydrogen bonds of the $^+$N—H$\cdots$S$^-$ type: N1—H1C$\cdots$S2^{iii} [(iii) $-y + \frac{3}{2}, x - \frac{1}{2}, z - \frac{1}{4}$] and N2—H2C$\cdots$S2^v [(v) $y, x, -z + 1$]. Interestingly, one can find the arrangements of the hydrogen bonds into distorted cubes laying at a twofold rotation axis, therefore having the C_2 Schoenflies group symmetry. The cubes (with alternating N and O atoms at vertices) are similar to those which have already been reported for the salts of some primary amines (Becker *et al.*, 2004). The difference in that case was the cubes did not form the network since monoamines were used. In the cube each of the N-vertices forms three bonds to three O-acceptors. The approximate symmetry of such an arrangement is $\bar{4}$, but the exact local symmetry is 2, so this might explain the selection of a Sohncke space group. Obviously the hydrogen bonding cubes are mutually interconnected by hydrocarbon chains, building the observed three-dimensional structure. The cubes can be labelled by atoms (N1, O3 together with rotation equivalents) at the top and (N2, O1 with equivalents) at the bottom 'square base' of the cube (Fig. 7). Disordered water molecules form O—H$\cdots$O$^-$ type bonds. Their positions are not well defined as the molecules are gathered near twofold rotation axes. H-atoms positions could not be determined from Fourier electron-density maps.

In the CSD (Version 5.37, February 2016) there are only 77 structures with the 1,5-diaminopentane dication (44 with three-dimensional coordinates determined). Among the structures 52 (67.5%) are organometallics. Among 44 structures six have several cations in the asymmetric unit, which gives 52 1,5-pentylenediaminium cation structures. 22 (42%) structures have the linear conformation of the carbon alkyl chain, other structures display varying degrees of folding with no preferences for other conformations. The histograms of the 1,5-pentylenediaminium cation structures deposited in the CSD are shown in Fig. S5. Among the compounds with the 1,5-pentylenediaminium cation, the largest number of structures have the greatest distances between the terminal C atoms but for the N$\cdots$N separation the conformational preference is not so well defined.

3.1.5. 1,6-hexylenediaminium thiosulfate. 1,6-Hexylenediaminium thiosulfate (5), $\{(H_3NC_6H_{12}NH_3)^{2+}, S_2O_3^{2-}\}_n$, crystallizes in the $P\bar{1}$ space group. The asymmetric unit contains two anions and two different cations. The first of the cations has a regular zigzag conformation, the second is bent and can be described by its torsions as (ap, ap, ap, sc, ap), with the sc angle (C7—C8—C9—C10) of 71.4 (8)$^\circ$. Separations of N atoms are 8.791 (7) and 8.116 (8) Å, for N1$\cdots$N2 and N3$\cdots$N4 and C$_{\alpha}\cdots$C$_{\omega}$ distances are 6.341 (9) and 5. 456 (9) Å for C1$\cdots$C6 and C7$\cdots$C12, respectively. The structure of (5) is shown in Fig. 8.

Similarly to (3), the plane regions of the hydrocarbon chains and hydrophilic regions of hydrogen-bonding interactions can be distinguished. Currently, for (5), the layers are parallel to the (011) plane. The hydrophilic areas are at $z = 0, 1, \ldots$, while hydrophobic areas are at $z = \frac{1}{2}, \frac{3}{2}$ *etc.* (Fig. 9). Apart from many chain and discrete hydrogen-bonding motifs, the characteristic ring motifs $R_4^2(8)$ are formed around symmetry centres. One motif, based on N2, O4^{iv} and their inversion-related counterparts is located at the centre ($\frac{1}{2} \frac{1}{2} \frac{1}{2}$), the second, based on N3 and O6^v and their counterparts, at ($0 \frac{1}{2} \frac{1}{2}$), the next based on N4 and O2^{vii} and their equivalents, at ($\frac{1}{2} 0 0$) while the last based on N1 and O1 lays around the (000) centre.

In the Cambridge Structural Database (Version 5.37, February 2016) 1,6-hexylenediaminium dication was found in 181 structures (115 with three-dimensional parameters refined). The number of structures is significantly larger than for those with the 1,5-pentylenediaminium cation, which could contribute to the availability and popularity of 1,6-diaminohexane being commonly used *e.g.* in polymer technology. This fact could also support the theory that compounds with an even number of C atoms in an alkyl chain crystallize relatively more readily (Paul & Kubicki, 2009). Among the 161 cation structures, 29 compounds deposited in the CSD have more
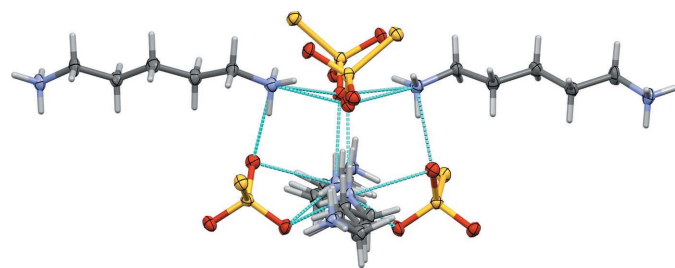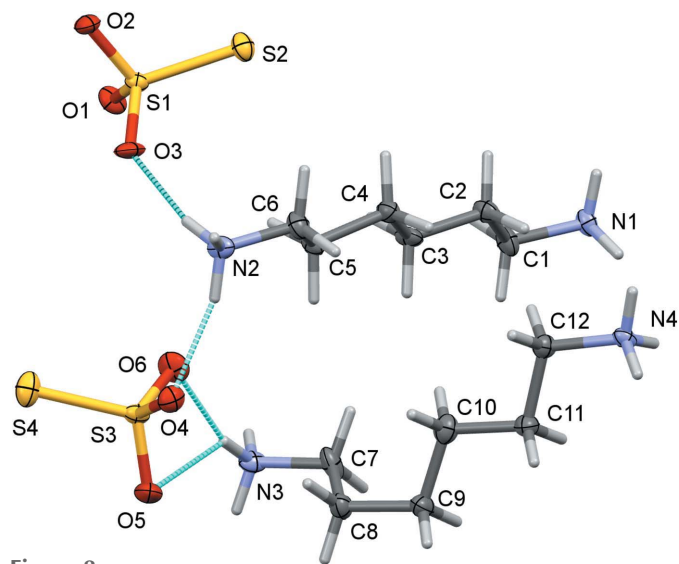

Figure 7
Hydrogen-bonding distorted cube with alternating N and O atoms at vertices – formed by four thiosulfate anions and four aminium cations in the structure of (4).

Figure 8
Molecular structure and atom-labelling scheme of 1,6-hexylenediaminium thiosulfate (5). Hydrogen bonds shown as dotted lines. Hanging hydrogen bonds are deleted. Ellipsoids drawn at the 50% probability level.

than one cation in the asymmetric unit, 97 (60%) have fully extended linear carbon alkyl chains. The distribution of conformations of the 1,6-hexanediaminium dication is shown in Fig. S6. In this case most of the structures also have a fully extended 1,6-hexylenediaminium cation, the second largest number of conformations is with one *sc* torsion angle, which is consistent with the conformations of two independent cations in 1,6-hexylenediaminium thiosulfate (5).

3.2. Discussion

The structures of compounds (2), (3) and (5) show the conformation of the cations can be frozen in a less favourable form if network Gibbs energy gain is profitable. DFT calculations of the energy difference in the various α,ω-alkyl-diaminium dication conformations conducted for (2) and (3) demonstrate the energy increase is quite small – approximately 12.6–16.7 kJ mol^{-1} (3–4 kcal mol^{-1}). According to the hierarchy of hydrogen-bonding energy, firstly the $^+$N—H$\cdots$O$^-$ type of bond is created, then the $^+$N—H$\cdots$S$^-$ type with much less energy. Similarly, in the structures with water molecules hydrogen bonds of the O—H$\cdots$O$^-$ type are more preferred than O—H$\cdots$S$^-$. The stabilization by $^+$N—H$\cdots$O$^-$ hydrogen bonds is strong enough to enforce less favourable conformations of the cations.

In order to investigate the intermolecular interactions in diaminium thiosulfates we calculated Hirshfeld surfaces and two-dimensional fingerprint plots using the *CrystalExplorer* software (Wolff *et al.*, 2013). Hirshfeld surface analysis gives information about the number of short contacts and does not reflect the energy of the interactions. Relative contributions of

intermolecular contacts to the Hirshfeld surface area for the compounds (1)–(5) are given in the supporting information (Figs. S7–S11). Results for all obtained compounds are very similar and reveal that for the anion more than 60% of the total interactions correspond to the O$\cdots$H interactions, with S$\cdots$H interactions above 30%. For the cation in the anhydrous structures the most prominent interactions are the H$\cdots$H short contacts, while H$\cdots$O and H$\cdots$S hydrogen-bond type interactions correspond to approximately 40% of the total interactions. In the hydrated structures for the cation H$\cdots$O and H$\cdots$H interactions are both equivalent to *ca* 45%, the remaining 10% are H$\cdots$S interactions. The Hirshfeld surface for the exemplary compound (1*b*) is shown in Fig. 10.

In the structures of (2), (3) and (5) we can observe two types of independent cations: one with a zigzag conformation and the second with a *gauche* conformation, which better suits the network of hydrogen bonding. NMR spectra reveal that in the solution α,ω-alkyldiaminium cations give the signals as the symmetrical compounds with no distinguished conformations (at room temperature).

It was found that an even number of C atoms in longer chains of α,ω-alkyldiaminium thiosulfates tends to induce the formation of structures with two-dimensional layers of hydrogen-bond domination and regions where only hydro-carbon chains are found. One can distinguish hydrophilic and hydrophobic alternating layered domains such as in compounds (3) and (5). In the alkyldiaminium thiosulfates with an odd number of C atoms in the hydrocarbon chain the structure of hydrogen bonding is three-dimensional with smaller cyclic motifs, but no layered domains are observed.

For the structures (1), (2) and (4) we obtained hydrates. All the compounds were synthesized by the same method under similar conditions, from water solutions, yet structures (3) and (5) are anhydrous. The prediction of the number of water molecules incorporated into the structure of diaminium thio-sulfates is difficult. Within the hydrated structures water molecules take part in robust hydrogen bond patterns, both as a donor and as an acceptor. Although the formation of the
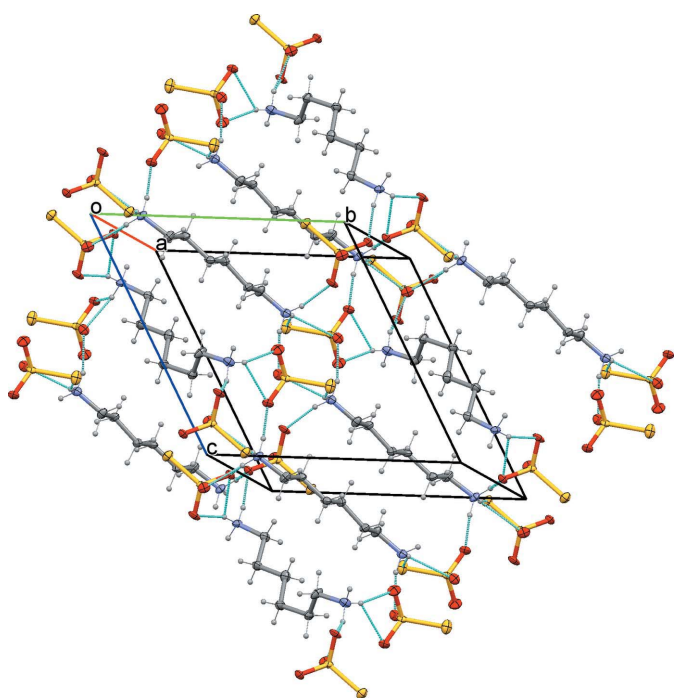

Figure 9
Packing diagram for (5). Alternate layered regions with hydrogen-bond domination, and with C—H chains only, are parallel to the (011) plane.
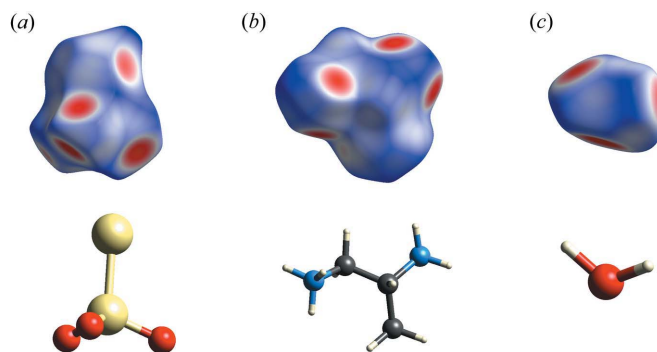

Figure 10
View of the Hirshfeld surfaces of (1*b*): (*a*) anion, (*b*) cation and (*c*) water molecule. Red colour – normalized contact distances d_{norm} shorter than the sum of van der Waals radii, blue colour – normalized contact distances exceeding the sum of van der Waals radii. Structures are shown at the bottom for guidance.

more extended hydrogen-bond network might be energetically profitable, the entropy change can cancel the gain and promote dehydrated structures.

The structure of (4), $\{(H_3NC_5H_{10}NH_3)^{2+}, S_2O_3^{2-}, \frac{1}{2}H_2O\}_n$, demonstrated that the formation of C_2 symmetric hydrogen-bonding patterns (distorted cube with alternating N, O vertices) may lead to a chiral structure. Crystallization of other aminium thiosulfates could induce spontaneous resolution. Starting from the racemic amine (±)-1,2-diaminopropane we obtained crystals of the enantiomeric salts [(1a) and (1b)] with the thiosulfate anion in good enantiomeric excess. Notably, all salts of the protonated 1,2-diaminoethane found in the CSD, which crystallized in Sohncke groups, contained a tetrahedral anion.

Song $et\ al.$ (2002) suggested that employing the α,ω-alkyl-diamine with an odd number of methylene C atoms as a structure-directing agent might induce the chirality of the resulting compounds. However, this hypothesis does not seem to be valid for compound (2) with three methylene C atoms which crystallizes in the centrosymmetric $P2_1/n$ space group. Also, Visi $et\ al.$ (2006) obtained a series of non-metal borates with linear α,ω-diaminoalkanes with a 5–12 carbon chain length which all crystallize in achiral groups. An overview of the CSD (Version 5.37, February 2016) shows that among compounds with the 1,3-propylenediaminium cation 32 structures (9%) crystallize in Sohncke space groups. This is significantly more than for the 1,4-butylenediaminium cation (7 structures, 3%) and 1,6-hexylenediaminium cation (14 structures, 8%). Among structures with the 1,5-pentyl-enediaminium cation 15 (19.5%) crystallize in chiral space groups, which can support the theory that salts of α,ω-alkyl-diamine with an odd number of methylene C atoms might crystallize in the Sohncke space groups more readily.

The question if one can deliberately obtain the spontaneous resolution or chiral structures starting from achiral components by utilizing robust charge-assisted hydrogen-bonding motifs is open.

4. Conclusions

By the reaction of ammonium thiosulfate with the corresponding diamine we obtained a series of diaminium salts and characterized them. The solid-state structures were determined for all obtained compounds. These experimental results, combined with data from the CSD, have shown that the formation of strong, charge-assisted hydrogen bonds influence many aspects of self-organization in the solid α,ω-alkyldiaminium thiosulfates. The hydrogen-bond patterns are quite complex and rigid, which in some cases enforce the less energetically favourable conformation of α,ω-alkyldiaminium cations [(2), (3) and (5)]. α,ω-Alkyldiaminium thiosulfates with an even number of methylene C atoms give structures with layered hydrogen-bond domains [(3) and (5)], while the salts with an odd number of C atoms in the aliphatic chain [(1a), (1b), (2) and (4)] form a three-dimensional type of hydrogen-bond network. In the structure of (4) hydrogen bonds arranged in the shape of distorted cubes, which are C_2

symmetric, could promote chiral structure ($P4_32_12$ space group). On the other hand, the reaction of racemic 1,2-di-aminopropane with $(NH_4)_2S_2O_3$ results in spontaneous resolution and obtains a conglomerate of crystals of 1,2-propylenediaminium thiosulfate of both enantiomers (1a) and (1b). The above examples show that achiral thiosulfate anions might induce the formation of chiral structures by hydrogen-bond interactions with the counterions.

References

Agilent Technologies (2013). $CrysAlisPro$. Santa Clara, USA.
Allen, F. H. (2002). $Acta\ Cryst.$ B58, 380–388.
Armstrong, R. S., Atkinson, I. M., Carter, E., Mahinay, M. S., Skelton, B. W., Turner, P., Wei, G., White, A. H. & Lindoy, L. F. (2002). $Proc.\ Nat.\ Acad.\ Sci.\ USA$, 99, 4987–4992.
Baouab, L. & Jouini, A. (1998). $J.\ Solid\ State\ Chem.$ 141, 343–351.
Becker, B., Baranowska, K., Chojnacki, J. & Wojnowski, W. (2004). $Chem.\ Commun.$ pp. 620–621.
Bernstein, J., Davis, R. E., Shimoni, L. & Chang, N.-L. (1995). $Angew.\ Chem.\ Int.\ Ed.\ Engl.$ 34, 1555–1573.
Blessing, R. H. (1997). $J.\ Appl.\ Cryst.$ 30, 421–426.
Bu, X., Gier, T. E., Feng, P. & Stucky, G. D. (1998). $Chem.\ Mater.$ 10, 2546–2551.
Budantseva, N. A., Andreev, G. B., Fedoseev, A. M. & Antipin, M. Y. (2003). $Russ.\ J.\ Coord.\ Chem.$ 29, 653–657.
Cheng, Z. & Lin, J. (2010). $CrystEngComm$, 12, 2646–2662.
Dąbrowska, A. & Chojnacki, J. (2014). $Z.\ Kristallogr.$ 229, 555–561.
Dumitrescu, D., Legrand, Y.-M., Petit, E., van der Lee, A. & Barboiu, M. (2014). $Chem.\ Commun.$ 50, 14086–14088.
Dumitrescu, D., Legrand, Y.-M., Petit, E., van der Lee, A. & Barboiu, M. (2015). $Chem.\ Sci.$ 6, 2079–2086.
Fang, G.-S., Sun, W.-Q., Zhao, W.-X., Lin, R.-L., Tao, Z. & Liu, J.-X. (2016). $Org.\ Biomol.\ Chem.$ 14, 674–679.
Farrugia, L. J. (2012). $J.\ Appl.\ Cryst.$ 45, 849–854.
Feng, P., Bu, X., Gier, T. E. & Stucky, G. D. (1998). $Microporous\ Mesoporous\ Mater.$ 23, 221–229.
Frisch, M. J. $et\ al.$ (2009). $GAUSSIAN$09. Gaussian, Inc., Wallingford CT, USA.
Gerrard, L. A. & Weller, M. T. (2002). $Acta\ Cryst.$ C58, m504–m505.
Guerfel, T. & Jouini, A. (2000). $J.\ Soc.\ Chim.\ Tunis.$ 4, 723–734.
Hunter, A. D. (1997). $J.\ Chem.\ Educ.$ 74, 905–906.
Jiang, T., Lough, A., Ozin, G. A. & Bedard, R. L. (1998). $J.\ Mater.\ Chem.$ 8, 733–741.
Knipe, P. C., Thompson, S. & Hamilton, A. D. (2015). $Chem.\ Sci.$ 6, 1630–1639.
Lee, C. & Harrison, W. T. A. (2003). $Acta\ Cryst.$ E59, m739–m741.
Lemmerer, A. & Billing, D. G. (2012). $CrystEngComm$, 14, 1954–1966.
Leyten, W., Rettig, S. J. & Trotter, J. (1988). $Acta\ Cryst.$ C44, 1749–1751.
Lopes Jesus, A. J. & Redinha, J. S. (2011). $J.\ Phys.\ Chem.\ A$, 115, 14069–14077.
Macrae, C. F., Bruno, I. J., Chisholm, J. A., Edgington, P. R., McCabe, P., Pidcock, E., Rodriguez-Monge, L., Taylor, R., van de Streek, J. & Wood, P. A. (2008). $J.\ Appl.\ Cryst.$ 41, 466–470.
Mitzi, D. B. (2004). $J.\ Mater.\ Chem.$ 14, 2355–2365.
Möller, K. & Bein, T. (2013). $Chem.\ Soc.\ Rev.$ 42, 3689–3707.
Okuniewski, A., Chojnacki, J., Baranowska, K. & Becker, B. (2013). $Acta\ Cryst.$ C69, 195–198.

Önal, M. & Sarıkaya, Y. (2008). *Colloids Surf. A Physicochem. Eng. Asp.* **312**, 56–61.

Parsons, S., Flack, H. D. & Wagner, T. (2013). *Acta Cryst.* B**69**, 249–259.

Paul, A. & Kubicki, M. (2009). *J. Mol. Struct.* **938**, 238–244.

Paul, A. & Kubicki, M. (2010). *J. Mol. Struct.* **966**, 107–112.

Pospieszna-Markiewicz, I., Zielaskiewicz, E., Radecka-Paryzek, W. & Kubicki, M. (2011). *Acta Cryst.* E**67**, o371–o372.

Seck, G. A., Sene, A., Diop, L. & Maris, T. (2016). *Acta Cryst.* E**72**, 273–275.

Sheldrick, G. M. (2008). *Acta Cryst.* A**64**, 112–122.

Song, H.-H., Yin, P., Zheng, L.-M., Korp, J. D., Jacobson, A. J., Gao, S. & Xin, X.-Q. (2002). *J. Chem. Soc. Dalton Trans.* pp. 2752–2759.

Srinivasan, B. R., Khandolkar, S. S., Jyai, R. N., Ravikumar, K., Sridhar, B. & Natarajan, S. (2013). *Spectrochim. Acta A Mol. Biomol. Spectrosc.* **102**, 235–241.

Srinivasan, B. R., Naik, A. R., Dhuri, S. N., Näther, C. & Bensch, W. (2011). *J. Chem. Sci.* **123**, 55–61.

Stoe & Cie GmbH (2015). *X-AREA*1.75. Stoe and Cie GmbH, Darmstadt, Germany.

Todd, M. J. & Harrison, W. T. A. (2005). *Acta Cryst.* E**61**, m2026–m2028.

Trabelsi, S., Essid, M., Roisnel, T., Rzaigui, M. & Marouani, H. (2014). *Acta Cryst.* E**70**, m84–m85.

Visi, M. Z., Knobler, C. B., Owen, J. J., Khan, M. I. & Schubert, D. M. (2006). *Cryst. Growth Des.* **6**, 538–545.

Wolff, S. K., Grimwood, D. J., McKinnon, J. J., Turner, M. J., Jayatilaka, D. & Spackman, M. A. (2013). *Crystal Explorer.* University of Western Australia, Australia.

Wong, L. W.-Y., Kan, J. W.-H., Nguyen, T., Sung, H. H.-Y., Li, D., Au-Yeung, A. S.-F., Sharma, R., Lin, Z. & Williams, I. D. (2015). *Chem. Commun.* **51**, 15760–15763.

Yang, Y.-X. & Ng, S. W. (2011). *Acta Cryst.* E**67**, o1664.

Yu, T., Zhang, L., Shen, J., Fu, Y. & Fu, Y. (2014). *Dalton Trans.* **43**, 13115–13121.

Zheng, S.-T., Zhang, J. & Yang, G.-Y. (2008). *Angew. Chem. Int. Ed.* **47**, 3909–3913.

Zhou, Y.-Y., Yao, S., Yan, J.-H., Chen, L., Wang, T.-T., Wang, C.-J. & Zhang, Z.-M. (2015). *Dalton Trans.* **44**, 20435–20440.